



0016-7037(94)E0023-E

Complexation of carbonate species at the goethite surface: Implications for adsorption of metal ions in natural waters

ALEXANDER VAN GEEN,* ALEXANDER P. ROBERTSON, and JAMES O. LECKIE
Department of Civil Engineering, Stanford University, Stanford, CA 94305, USA

(Received June 25, 1993; accepted in revised form January 10, 1994)

Abstract—Headspace P_{CO_2} was measured with an infrared gas analyzer over an equilibrated goethite suspension to determine adsorption of carbonate species in the pH range 3 to 8. For a 2 g/L goethite suspension in 0.1 N NaClO_4 ($\sim 3 \cdot 10^{-4}$ M surface sites), the fraction of carbonate species adsorbed increased from 0.15 at pH 3 to a maximum of 0.56 at pH 6. In 0.01 N NaClO_4 , the fraction of carbonate species adsorbed at pH 6 increased to 0.67. The total concentration of CO_2 in the suspension increased from about 0.4 to $0.6 \cdot 10^{-4}$ M in the pH range of these experiments. The development of surface charge at the goethite surface was determined in the pH range 4 to 11 by potentiometric titration under controlled low CO_2 conditions. No hysteresis was observed between the acid and base legs of titrations in 0.10, 0.03, and 0.01 N NaClO_4 resulting in a pH_{pzc} of 8.9. The carbonate species adsorption data were modelled using the least squares optimization program FITEQL for the diffuse double-layer model and the triple-layer model using stoichiometries of the type Fe-OCOOH and Fe-OCOO^- for surface bound carbonate species. The model results are consistent with separate experiments showing a significant reduction in chromate adsorption on goethite as the partial pressure of CO_2 was increased from <5 to 450 and 40,000 μatm . Our data suggest that mineral oxide surface sites which control solid/solute partitioning of metal ions in natural systems may be largely bound to adsorbed carbonate species.

INTRODUCTION

THE CONCENTRATION OF metal ions dissolved in natural waters is largely determined by the availability of surface sites for adsorption (HEM, 1970; TUREKIAN, 1977). While concentrations of dissolved Al, Fe, and Mn on the order of 10^{-6} M in fresh waters may be determined in some cases by equilibria with silicate and oxide phases of these elements, adsorption onto mineral oxides is generally thought to limit concentrations of Cd, Cu, Ni, Zn, and other trace elements to 10^{-9} M levels (SHILLER and BOYLE, 1987). To better understand adsorption processes at a fundamental level, many laboratory studies of the surface properties of mineral surfaces such as iron and manganese oxides, silicates, and carbonates have been conducted (e.g., BENJAMIN, 1983; DAVIS et al., 1978; DAVIS and LECKIE, 1978, 1980; HAYES and LECKIE, 1987; HAYES et al., 1988; FULLER and DAVIS, 1987; ZACHARA et al., 1987; WIELAND and STUMM, 1992; VAN CAPPELLEN et al., 1993). Potentiometric titrations of solid suspensions have demonstrated that protonation and deprotonation reactions occur at oxide surfaces (HUANG and STUMM, 1973; YATES and HEALY, 1975; JAMES and PARKS, 1982). The pH dependence of metal adsorption in batch studies under different conditions has also been used to interpret the behaviour of a number of metal ions (BENJAMIN and LECKIE, 1982). More recently, spectroscopic studies have been used to probe the nature of bonds formed between surface moieties and solution species (HAYES et al., 1987; CHISHOLM-BRAUSE et al., 1990; ROE et al., 1991; COMBES et al.,

1992). The extrapolation of the above studies to metal adsorption in natural systems has proven difficult (SCHINDLER and STUMM, 1987; DAVIS and KENT, 1990).

If adsorption is attributed to the formation of a bond between a specific functional group at the oxide surface and a solution species, then adsorption becomes a reaction competing for metal ions with other ligands in solution (BOURG and SCHINDLER, 1978). A quasi-thermodynamic description of surface complexation reactions can then be combined with the known solution chemistry of various metal ions to predict adsorption over a range of conditions (SPOSITO, 1984). Metal adsorption has been measured in electrolytes such as NaCl, KCl, NaNO_3 , and NaClO_4 . The dependence of adsorption on solution ionic strength is an object of study because metal oxide surfaces are typically charged and surface complexation is, therefore, sensitive to the structure of the electrical double layer at the oxide-solution interface (HAYES and LECKIE, 1987; HAYES et al., 1988). One still unresolved important issue is the extent to which major ions in continental waters such Ca^{+2} , Na^+ , Cl^- , Mg^{+2} , and SO_4^{2-} (e.g., HOLLAND, 1978) bind specifically to oxide surfaces and compete for surface sites with other metal ions present at much lower concentrations. Only a limited number of studies dedicated to a specific trace element have examined the adsorption of the major ions on the same surface in parallel (BALISTRERI and MURRAY, 1982, 1983; ZACHARA et al., 1987). The adsorption behaviour of carbonate species, often a dominant solute in continental waters, has been largely neglected with the exception of the work RUSSELL et al. (1974), SHULTHESS and MCCARTHY (1990), and ZACHARA et al. (1987). More recently, BRUNO et al. (1992) postulated the formation of a bicarbonate surface complex for another iron oxide, hematite, to explain the dissolution kinetics of this solid in the presence

* Present address: Lamont-Doherty Earth Observatory of Columbia University, Palisades, NY 10964, USA and USGS, MS 465, Menlo Park, CA 94025, USA.

of CO_2 . To our knowledge, the present paper contains the first study amenable to surface complexation modelling of carbonate species adsorption onto goethite, a metal oxide ubiquitous in soils and streams (SPOSITO, 1989). Our data suggest that adsorbed carbonate complexes may sharply reduce the ability of metal oxide surface sites to bind trace metals at CO_2 partial pressures and pH values typical for soils and groundwater.

Acidic and alkaline environments must be distinguished to determine the range of carbonate concentration in natural waters. The dominant species in solution below and above pH 6 are carbonic acid H_2CO_3^* ($\text{CO}_{2\text{aq}}$) and the bicarbonate ion HCO_3^- , respectively (STUMM and MORGAN, 1981). In this paper the term carbonate species includes both. A lower limit of 10 μM carbonate in solution can be calculated for soil water at $\text{pH} < 6$ from the partial pressure of CO_2 in the atmosphere of 350 μatm and Henry's law constant of K_h of $10^{-1.47}$ mol/L atm^{-1} at 25°C (HARNED and DAVIS, 1943). As noted by SPOSITO (1989), however, the CO_2 content of soil air typically ranges between 3,000 and 30,000 μatm . A more reasonable concentration range for carbonate species in acidic aqueous environments is therefore 100–1000 μM . At $\text{pH} > 7$, the concentration of carbonate species in equilibrium with the atmosphere rises by an order of magnitude for every unit of pH increase. A useful reference is seawater in equilibrium with atmosphere at pH 8.3 which contains about 2000 μM carbonate in solution (STUMM and MORGAN, 1981). Comparable levels of dissolved carbonate have been measured in groundwater (HEM, 1970). Carbonate levels in continental waters are therefore comparable to the concentrations of the major ions Ca^{+2} , Na^+ , Cl^- , Mg^{+2} , and SO_4^{2-} .

EXPERIMENTAL

Preparation of Goethite

Goethite was prepared from reagent grade ferric nitrate and sodium hydroxide using a slightly modified version of the method described by ATKINSON et al. (1967). 450 g of ferric nitrate ($\text{Fe}(\text{NO}_3)_3 \cdot 9\text{H}_2\text{O}$) was dissolved in 8.3 L of Milli Q water (CO_2 reduced by boiling). 900 mL of low carbonate 5 N NaOH was added and mixed with the ferric nitrate solution while keeping an Ar purge in the headspace. The base addition brought the pH to around 12. The polypropylene container was capped and the solution kept in an oven for 24 h at 60°C. The goethite solution was then placed in trace-metal-free dialysis tubing (Spectra por 7) and dialyzed against Milli Q water. The water was changed once or twice a day and the conductivity of the spent water was measured. This process was continued for two to three changes past the point where the conductivity of a solution in contact with the goethite for one day was 1–2 μS . Ten batches of goethite were made in this manner, mixed and stored as a slurry (~120 g goethite per liter) in a polypropylene container at 4°C. 40 g/L working solutions were made by diluting this stock. XRD measurements confirmed that the synthesized material was goethite. Surface area determination by nitrogen adsorption on the dried powdered goethite yielded a value of 45 (± 2) m^2/g (BRUNAUER et al., 1938).

Potentiometric Titrations

All titrations were conducted on 100 mL suspensions of 10.0 g/L goethite in a Teflon vessel placed in waterjacket reactor and kept under argon at 25°C. The computer-controlled apparatus and associated titration protocols are described in detail elsewhere (A. P. Robertson, unpubl. data). The samples were prepared from a stock solution at 0.002 N ionic strength and acidified to somewhere between pH 4.5–5.0. To minimize solution CO_2 , the stock solution was sparged

with Ar for 10–20 h and stored at 4°C in a ground glass stoppered Erlenmeyer flask. Appropriate volumes of concentrated NaClO_4 solution and low CO_2 Milli Q water were combined with the stock solution to reach the desired volume, concentration, and ionic strength. Titrations were run from the initial pH up to pH 10.7–11, down to pH 3.8–4, and back to the starting pH. Data was collected at ~0.2 pH unit intervals. Equilibrium was assumed to occur when pH drift was less than 0.01 mV/min in the pH 6–8 region and 0.005 mV/min otherwise (drift of less than 0.01 pH units/h). Elapsed time between data points ranged from 5–40 min. Complete titrations containing sixty to ninety data points required 16–24 h.

Description of the CO_2 Equilibration Device

The main components of the headspace equilibration system are shown in Fig. 1. The cylindrical glass vessel (total volume including pump and tubing: 268.5 mL) is equipped with gas tight fittings to allow the introduction of a pH probe (Orion, Ross combination microelectrode), a glass gas dispersion tube, and a 2.5 mL capacity microburet (Gilmont Instruments, Inc.). The coupling for a silicon septum can also be opened for changing the suspension and cleaning system. The headspace gas is recirculated through the suspension at 250 mL/min with a small stainless steel diaphragm pump (Spectrex Inc., Redwood City, CA). The pump-head required extensive coating with epoxy to prevent gas exchange with the surroundings. The electric motor also had to be replaced because the original motor axle could not sustain the additional resistance caused by a silicone layer applied over the viton pump baffles to reduce gas diffusion. Two stainless steel gas chromatography valves (Valco) and two brass 3-way toggle

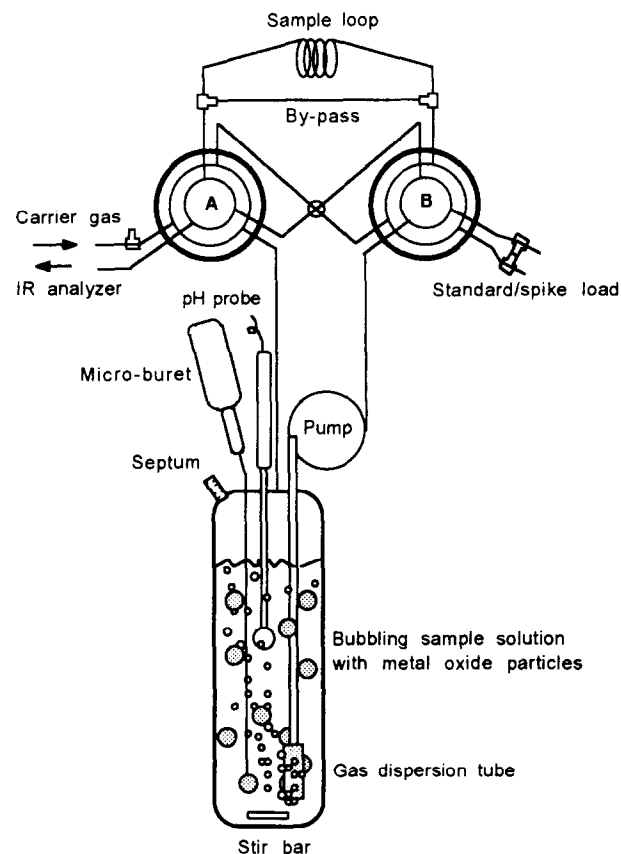


FIG. 1. Equilibration vessel used to measure headspace CO_2 in equilibrium with the goethite suspension as a function of pH. Headspace air is recirculated by the pump through the goethite suspension and sample loop system that is isolated from its surroundings. The carrier gas flows directly to the IR analyzer. By switching the two valves A and B simultaneously, the content of the sample loop is placed in-line with the carrier gas path leading to the IR analyzer.

valves (Minimetrics, Clippard) were interconnected by $\frac{1}{8}$ " copper tubing to allow switching between the different configurations of the device: (1) closed-system recirculation, (2) purging of system with CO₂-free air on-line, (3) injection of sample loop content to the IR analyzer, and (4) loading of standard in sample loop for calibration/loading of CO₂ spike to equilibration vessel. Configuration (3) switches the 3.06 mL sample loop in-line to a Horiba PIR-2000 non-dispersive infrared gas analyzer via a drying tube (MD-250-24P, Perma Pure Dryer, Toms River, NJ). For the chosen combination of sample loop size and flow rate (CO₂-free carrier gas: 20% O₂, 80% N₂), IR absorption was linear up to 2000 μ atm P_{CO_2} with a detection limit of 5 μ atm. Precision based on repeated injection of 1000 and 500 μ atm CO₂ calibration gases in nitrogen (Scotty II, Alltech, Deerfield, IL) was better than 0.5% and instrument drift during the course of a day was undetectable.

Measurement of CO₂ Adsorption

The sample loop was first loaded with 10.090% CO₂ in nitrogen for later inclusion in the recirculation flowpath ($1.26 \cdot 10^{-5}$ mol total CO₂ added). Suspensions of 10, 2, and 0 g/L goethite in 0.1 N NaClO₄ (volume: 200 mL) were then purged of CO₂ by bubbling the carrier gas through the equilibration system for $\sim\frac{1}{2}$ h at pH 3. During the purging interval, headspace CO₂ equilibrated with the suspension decreased from >2000 μ atm to below the detection limit of 5 μ atm. The elevated amount of CO₂ initially adsorbed on the goethite surface is not surprising since the goethite stock solution stored at pH \sim 9 is presumably in equilibrium with ambient air. After brief decompression of the vessel via the on-line toggle valve, the system was closed by including the content of the sample loop containing the CO₂ spike and equilibrated by recirculating the headspace through the suspension for 5 min. Longer recirculation times did not change headspace CO₂ indicating equilibrium distribution was reached rapidly. After stopping the pump and waiting one minute to allow the pressure to equalize throughout the recirculation circuit, the circuit outside the sample loop was first purged by switching it in-line with the carrier gas flowing to the IR analyzer. Two toggle valves were then switched simultaneously for introduction of the sample loop content to the IR analyzer. Following a headspace measurement, the sample loop was reintroduced to the equilibration system after brief decompression of the carrier gas. The pH is increased stepwise between each headspace measurement by addition of 1 N NaOH with a microburet (total addition of \sim 0.3 mL). When a headspace P_{CO_2} of \sim 50 μ atm was reached at the end of an experiment, mass-balance of the system was checked by bringing the solution pH to 3 with acid delivered via a syringe needle through the septum. The CO₂ contribution from NaOH additions was determined separately by incremental additions of base to a 0.1 N NaClO₄ solution at pH 2 in the equilibration device followed by equilibration and headspace CO₂ determination. Even with carefully prepared "carbonate-free" NaOH and boiled Milli Q water, dissolved CO₂ in the 1 N NaOH solution was \sim 1.3 $\cdot 10^{-3}$ M. Contributions from this source amounted to at most 4% of the total CO₂ present in the system. P_{CO_2} at pH 3 at the end of each experiment was within 93–99% of the initial value when corrected for CO₂ contributions from the base and CO₂ removal via the sample loop for each measurement.

Chromate Adsorption

In contrast to the procedure above, chromate adsorption was determined in an open carbonate system at three partial pressures of CO₂: <5, 450, and 40,000 μ atm. A 200 mL goethite suspension (10 g/L) in 0.1 N NaClO₄ was set up in a glove bag (AtmosBag, Aldrich Chemical Co., Milwaukee) inflated by a steady stream of O₂/N₂ with CO₂ at \leq 5 and 40,000 μ atm, respectively. Laboratory air was used for the experiment at the intermediate P_{CO_2} level of 450 μ atm (slightly higher than typical outdoor atmospheric value of 350 μ atm). The goethite suspension was first equilibrated by bubbling glove bag or laboratory air for 1 h with the same dispersion tube and pump assembly used for the closed vessel experiments. The initial pH of the goethite suspension of 8.3 was reduced to 5.4 and 7.5, respectively, by equilibration with 40,000 and 450 μ atm P_{CO_2} . For these two experiments, a saturated (0.5 M) NaHCO₃ solution was added to increase pH and total carbonate simultaneously in the suspension. This

reduced the time required to reach carbonate equilibrium as indicated by little pH drift within \sim 10 min after addition of the NaHCO₃ buffer. At each pH interval, 10 mL of the goethite suspension was transferred to 30 mL polycarbonate centrifuge tubes. A 100 μ L spike of pre-mixed Na₂CrO₄ and ⁵¹Cr tracer was added to each tube to bring total concentrations to 5 $\cdot 10^{-6}$ M Cr (VI) and \sim 50 cpm/mL, respectively. After rotation within the glove bag/laboratory atmosphere for 2 h, the tubes were reopened and pH was measured again while stirring the suspension. In all cases, the drift between the end of carbonate equilibration and the 2 h rotation was below 0.1 pH units. P_{CO_2} monitored in the glove bag remained < the 5 μ atm detection limit throughout the "carbonate-free" experiment. Here, a few drops of acid were added to the carbonate-free solution to lower the initial pH to 6.0, and a microburet containing 1 N NaOH was used to subsequently raise the pH of the suspension (total of 0.2 mL added). After the second pH measurement, tubes were capped and removed from the glove bag for centrifugation at 3700 rpm for 10 min. The clear supernatant (8 mL) was transferred to scintillation vials for counting for 30 min on a Packard Minimax 5000 Series gamma-counter.

RESULTS

Potentiometric Titrations

Goethite particles in a suspension act as a buffer during potentiometric titrations due to proton uptake and release by surface hydroxyl groups. Surface charge can be calculated from the measured pH and acid/base added at each data point (Appendix A) and the electroneutrality condition for the suspension:

Surface charge concentration

$$= (C_a - C_b) - ([\text{H}^+] - [\text{OH}^-]), \quad (1)$$

where C_a and C_b denote moles of acid/base added and [] stand for concentrations. Using Faradays constant (96,480 C/mol of charge), the dissociation constant of water, activity coefficients for charged solution species, and the surface area for this batch of goethite, the change in surface charge density as a function of pH can be calculated from the titration data (Fig. 2). The goethite surface is positively charged over the typical pH range of natural waters and the buffering capacity of a goethite suspension increases with ionic strength. It is important to note that no hysteresis was observed between the acid and base legs of the titrations. The cross-over point of surface charge data at different background electrolyte concentrations coincide at the point of no net acid/base addition to the suspension, pH 8.9. The interpretation of this common point, often called the point of zero charge (pHpzc) depends on whether or not background electrolyte binding to the surface is thought to be significant. If electrolyte binding is negligible (or exactly symmetrical), protonated and deprotonated surface sites Fe-OH₂⁺ and Fe-O⁻ are in balance at the pHpzc which is then also called the pristine point-of-zero charge, pHppzc (DAVIS and KENT, 1990). If, on the other hand, electrolyte binding is significant and possibly not symmetric around the pHpzc, zero net charge at the pHpzc reflects charge balance between protonated and deprotonated surface sites taking into account formation of surface complexes such as Fe-OH₂⁺-ClO₄⁻ and Fe-O⁻-Na⁺.

CO₂ Adsorption

The rapid decrease in headspace P_{CO_2} over the electrolyte solution in the absence of goethite at pH > 5.5 reflects the

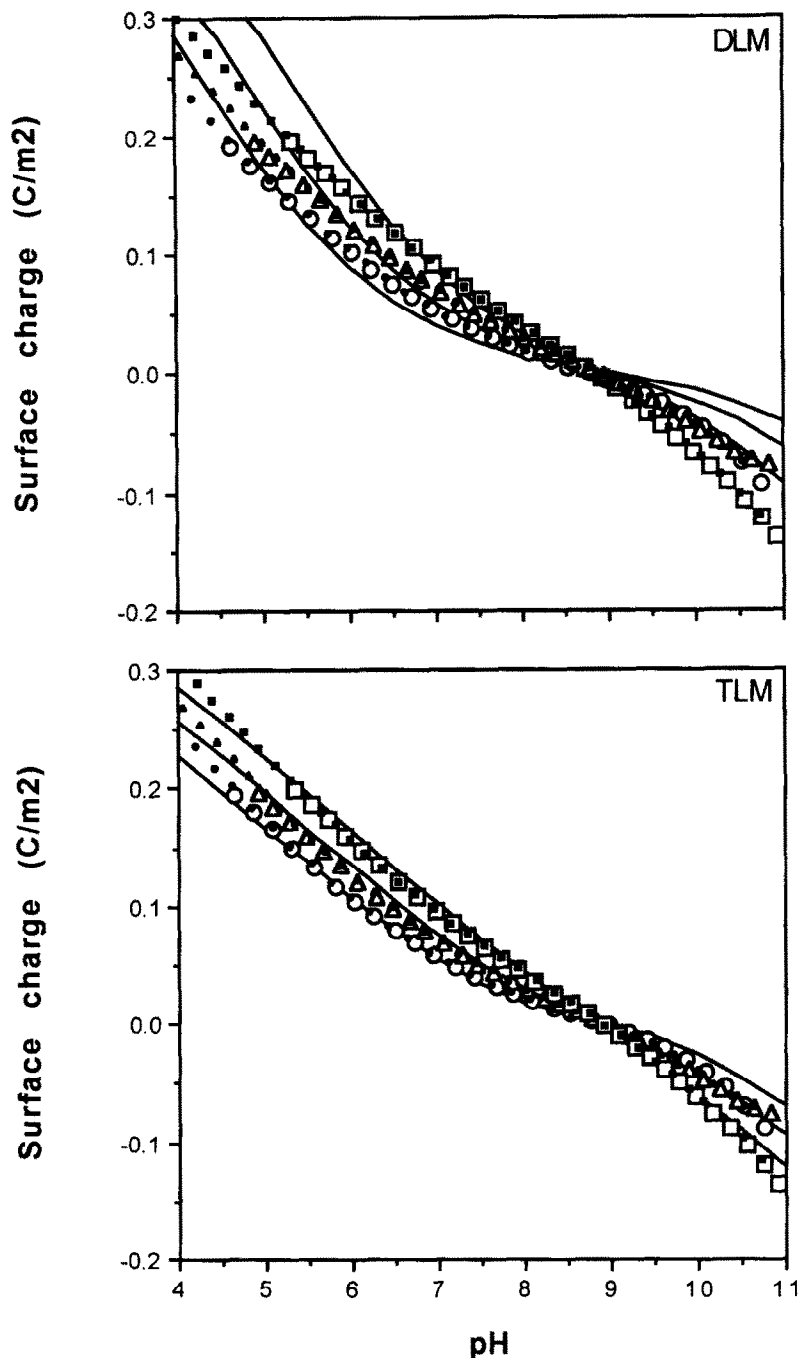


FIG. 2. Variation in surface charge density as a function of pH calculated from Eqn. 1 and the potentiometric data in Appendix A. 10 g/L suspension of goethite. Ionic strength of NaClO_4 electrolyte: 0.1 N (square symbols), 0.03 N (triangles), and 0.01 N (circles). Overlapping large and small symbols refer to the base and acid legs of the titration, respectively. Comparison of data to predicted variations in surface charge density according to formation constants listed in Table 1 for diffuse layer model (upper panel) and triple-layer model (lower panel).

dissociation of carbonic acid to bicarbonate (Fig. 3). The data compare very well with P_{CO_2} predicted from the total amount of CO_2 added to the system, solution and headspace volume, and carbonate chemistry. Carbonate solution species considered in this calculation and their formation constants are listed in Table 1. The effective Henry's Law coefficient $K_h = 10^{-1.465}$ required to match model and data at $\text{pH} < 5$ is only slightly higher than the coefficient interpolated to 0.1

N ionic strength of HARNED and DAVIS (1943). Evidently, the solution was 3% supersaturated relative to headspace P_{CO_2} which is not surprising since the bubbles were recirculated into the solution at ~ 15 cm depth. The main conclusion from this comparison is that the equilibration system was well sealed and standard carbonate chemistry was closely followed. When the same CO_2 spike was added to 2 and 10 g/L goethite suspensions, respectively, headspace P_{CO_2} was

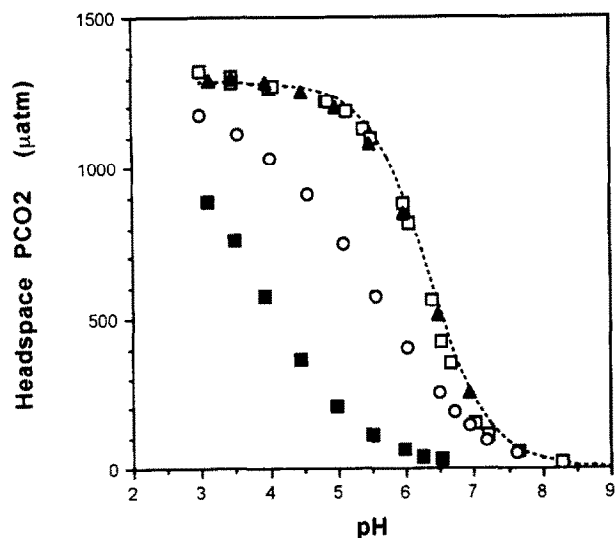


FIG. 3. Headspace P_{CO_2} in headspace of the equilibration device measured by infrared absorption for 2 g/L (open circles) and 10 g/L (filled squares) goethite suspensions in 0.1 N NaClO_4 . Dotted line shows the predicted pH dependence of P_{CO_2} based on the geometry of the device and standard carbonate chemistry. Headspace data included for solid free solution (open squares) and the Cr VI saturated (10^{-2} M) 10 g/L goethite suspension (triangles).

clearly reduced relative to the solid free case throughout the pH range 3 to 7 (Fig. 3). One initial concern with this approach to measure carbonate species binding was that the gas exchange properties of the solution might be affected by the goethite particles. Bubble size in the equilibration vessel during recirculation decreased with increasing suspended solid concentrations, for instance. To test this possibility, a sufficient amount of Na_2CrO_4 was added to a 10 g/L goethite suspension in 0.1 N NaClO_4 to effectively saturate the solid surface with chromate over the 3 to 7 pH range and the same experiment was repeated. Total Cr (VI) in the suspension of $1.0 \cdot 10^{-2}$ M Cr (VI) can be compared to $\sim 0.2 \cdot 10^{-2}$ M surface sites calculated from a surface site density of 2.3 sites/ nm^2 (DAVIS and KENT, 1990, see discussion). Figure 3 shows that P_{CO_2} equilibrated with the chromate-saturated goethite suspension behaved very much like the solid-free solution. This demonstrates that the solid suspension did not significantly affect gas exchange properties in the equilibration device and confirms that P_{CO_2} reductions over 2 and 10 g/L suspensions relative to the solid-free case truly reflect adsorption of carbonate species on the goethite surface.

The headspace data can be used to calculate the fraction of total CO_2 in the suspension adsorbed onto goethite as a function of pH. An interpolated curve based on the solid-free data was used to establish the relation between headspace P_{CO_2} and the total CO_2 in solution at any pH for the system. This approach was chosen to avoid errors due to small systematic deviations from thermodynamic predictions visible in Fig. 3. This empirical relation which is independent of the amount of solid present was used to graphically determine total CO_2 in solution from the headspace concentration at each pH. Knowing the moles of carbon dioxide added to the system $\text{CO}_{2(\text{tot})}$, the amount in the headspace $\text{CO}_{2(\text{head})}$ from

the IR measurement (gas molar volume of 24.5 L/mol at 25°C), and the amount in solution from the empirical headspace- $\text{CO}_{2(\text{sol})}$ relation, the fraction of total CO_2 in the suspension adsorbed onto the solid can be calculated:

Fraction adsorbed of CO_2 in suspension

$$= \frac{\text{CO}_{2(\text{tot})} - \text{CO}_{2(\text{head})} - \text{CO}_{2(\text{sol})}}{\text{CO}_{2(\text{tot})} - \text{CO}_{2(\text{head})}} \quad (2)$$

Results from this expression are shown in Fig. 4 including error bars calculated by propagating an estimated ± 8 μatm uncertainty in the difference between P_{CO_2} over a goethite suspension and the solid-free solution. Errors bars on the fraction adsorbed become significant at $\text{pH} > 6.5$ because the relative effect of this uncertainty increases rapidly as the absolute difference between suspension and solid-free data diminishes (Fig. 3). For a 2 g/L goethite suspension, the fraction of carbonate species adsorbed increased from 0.13 at pH 3 to a maximum of 0.56 at pH 6 (Appendix B). Despite widening error bars, the fraction adsorbed clearly decreased for $\text{pH} > 6$. As expected, the fraction adsorbed in 10 g/L goethite suspension was higher throughout the pH range and reached a plateau of 0.95 at pH 6. An unavoidable consequence of measuring carbonate adsorption by this method is that the total CO_2 concentration in the suspension increases from about 40 to 60 10^{-6} M between pH 5 and 8 (Fig. 4). Calculating the fraction adsorbed of total CO_2 in the suspension from Eqn. 2 takes this into account. The maximum surface site coverage by adsorbed carbonate species in the 2 and 10 g/L goethite suspensions was 9 and 3%, respectively, assuming a site density of 2.3 sites/ nm^2 and monodentate binding.

Headspace P_{CO_2} as a function of pH was also measured for a solid-free and 2 g/L goethite solution in 0.01 N NaClO_4 to determine the effect of ionic strength on carbonate species adsorption. Initial headspace CO_2 at pH 3 for the solid-free solution in 0.01 N electrolyte (not shown) was slightly lower than for 0.1 N NaClO_4 (1250 vs. 1300 μatm) due to the expected ionic strength effect on partitioning (HARNED and DAVIS, 1943). At $\text{pH} > 5.5$ on the other hand, P_{CO_2} remained slightly higher than during the 0.1 N experiment due to the higher activity coefficient of bicarbonate in 0.01 N NaClO_4 (0.78 vs. 0.90). The 0.01 N ionic strength data was also converted following Eqn. 2 to determine the fraction of total CO_2 in the suspension adsorbed as a function of pH and is included in Fig. 4 with the 0.1 N ionic strength results. The fraction adsorbed increased from 0.56 in 0.1 N to 0.67 at pH 6 in 0.01 N NaClO_4 (Appendix B).

Chromate Adsorption

The set of chromate adsorption experiments as a function of pH at different partial pressures of CO_2 serves as an independent test of the role of carbonate species in modifying the properties of a metal oxide surface such as goethite (Appendix C). Because carbonate species binding could not be measured precisely with the configuration of the equilibration device at $\text{pH} > 7$, the chromate data also constrain the role of carbonate species in the pH range more typical of ground-

TABLE 1. Formation constants of species considered in modelling the goethite surface, carbonate adsorption, and chromate adsorption

In Solution		
Components H^+ , Na^+ , CO_3^{2-} , CrO_4^{2-}		
K_{OH^-}	$= a_1 [OH^-] a_1 [H^+]$	$= 10^{-13.99}$
$K_{HCO_3^-}$	$= a_1 [HCO_3^-] / a_1 [H^+] a_2 [CO_3^{2-}]$	$= 10^{10.33}$
$K_{H_2CO_3}$	$= [H_2CO_3] / (a_1)^2 [H^+]^2 a_2 [CO_3^{2-}]$	$= 10^{16.68}$
$K_{NaCrO_4^-}$	$= a_1 [NaCrO_4^-] / a_1 [Na^+] a_2 [CrO_4^{2-}]$	$= 10^{0.70}$
$K_{HCrO_4^-}$	$= a_1 [HCrO_4^-] / a_1 [H^+] a_2 [CrO_4^{2-}]$	$= 10^{6.51}$
On goethite surface with diffuse-layer model		
Additional component, Fe-OH		
$K_{Fe-OH_2^+}$	$= [Fe-OH_2^+] \exp(F\Psi_0/RT) / [Fe-OH] a_1 [H^+]$	$= 10^{7.91}$
K_{Fe-O^-}	$= [Fe-O^-] a_1 [H^+] \exp(-F\Psi_0/RT) / [Fe-OH]$	$= 10^{-10.02}$
$K_{Fe-OCOOH}$	$= [Fe-OCOOH] / [Fe-OH] (a_1)^2 [H^+]^2 a_2 [CO_3^{2-}]$	$= 10^{20.78}$
$K_{Fe-OCOO^-}$	$= [Fe-OCOO^-] \exp(-F\Psi_0/RT) / [Fe-OH] a_1 [H^+] a_2 [CO_3^{2-}]$	$= 10^{12.71}$
$K_{Fe-OH_2^+-CrO_4^{2-}}$	$= [Fe-OH_2^+-CrO_4^{2-}] \exp(F\Psi_0/RT) / [Fe-OH] a_1 [H^+] a_2 [CrO_4^{2-}]$	$= 10^{12.75}$
On goethite surface with triple-layer model ($C_1=1.5$ and $C_2=0.2$ F/m ²)		
Additional components, Fe-OH, ClO_4^-		
$K_{Fe-OH_2^+}$	$= [Fe-OH_2^+] \exp(F\Psi_0/RT) / [Fe-OH] a_1 [H^+]$	$= 10^{7.90}$
K_{Fe-O^-}	$= [Fe-O^-] a_1 [H^+] \exp(-F\Psi_0/RT) / [Fe-OH]$	$= 10^{-9.90}$
$K_{Fe-OH_2^+-ClO_4^-}$	$= [Fe-OH_2^+-ClO_4^-] \exp(F(\Psi_0-\Psi_\beta)/RT) / [Fe-OH] a_1 [H^+] a_1 [ClO_4^-]$	$= 10^{8.89}$
$K_{Fe-O^-Na^+}$	$= [Fe-O^-Na^+] a_1 [H^+] \exp(F(\Psi_\beta-\Psi_0)/RT) / [Fe-OH] a_1 [Na^+]$	$= 10^{-8.76}$
$K_{Fe-OCOO^-}$	$= [Fe-OCOO^-] \exp(-F\Psi_0/RT) / [Fe-OH] a_1 [H^+] a_2 [CO_3^{2-}]$	$= 10^{12.45}$
$K_{Fe-CrO_4^-}$	$= [Fe-CrO_4^-] \exp(-F\Psi_0/RT) / [Fe-OH] a_1 [H^+] a_2 [CrO_4^{2-}]$	$= 10^{12.82}$

[] denote concentrations; a_1 , a_2 activity coefficients for single and double charged ions

F: Faraday's constant (96,485 C/mole of e^-)

Ψ_0 , Ψ_β surface potentials at the 0 and β planes, respectively.

Properties of goethite: Surface area 45 m²/g

Site density 2.3 sites/nm²

water. Figure 5 shows the usual decrease in fraction adsorbed with increasing pH expected for an anion such as CrO_4^{2-} (DAVIS and LECKIE, 1980). More interesting is the observation that the pH of 50% adsorption of chromate is lowered from 9.4 under essentially carbonate-free conditions to 8.8 when a 10 g/L suspension of goethite is equilibrated with laboratory air (450 μ atm). At P_{CO_2} of 40,000 μ atm, the pH of 50% adsorption of chromate is shifted further down to 7.8. Note that in these open-system experiments, total CO_2 in solution increases rapidly with higher pH. The change in suspension CO_2 concentration calculated assuming equilibration with laboratory air (450 μ atm) or glove-bag air (40,000 μ atm) is included in Fig. 5. The equilibrium assumption is justified by our experience using the same dispersion tube and pump combination for the closed system. The sensitivity of chromate adsorption to P_{CO_2} confirms that

precautions must be taken to control CO_2 transfer during batch metal adsorption experiments at pH higher than 7.

DISCUSSION

Characterization of the Goethite Surface

Previous determinations of the point of zero charge for goethite vary over a wide range: $pH_{pzc} = 7.3$ in $NaClO_4$ according to ATKINSON et al. (1967); $pH_{pzc} = 8.45$ in $NaNO_3$ (HAYES et al., 1987); and $pH_{pzc} = 9.0 \pm 0.3$ in $NaClO_4$ (ZELTNER and ANDERSON, 1988). To some extent, the discrepancies may be due to different binding intensities to the goethite surface by the electrolytes ions. A comparison of titration data for goethite suspension purged and unpurged of CO_2 by ZELTNER and ANDERSON (1988), however, strongly suggests that earlier low pH_{pzc} values may largely

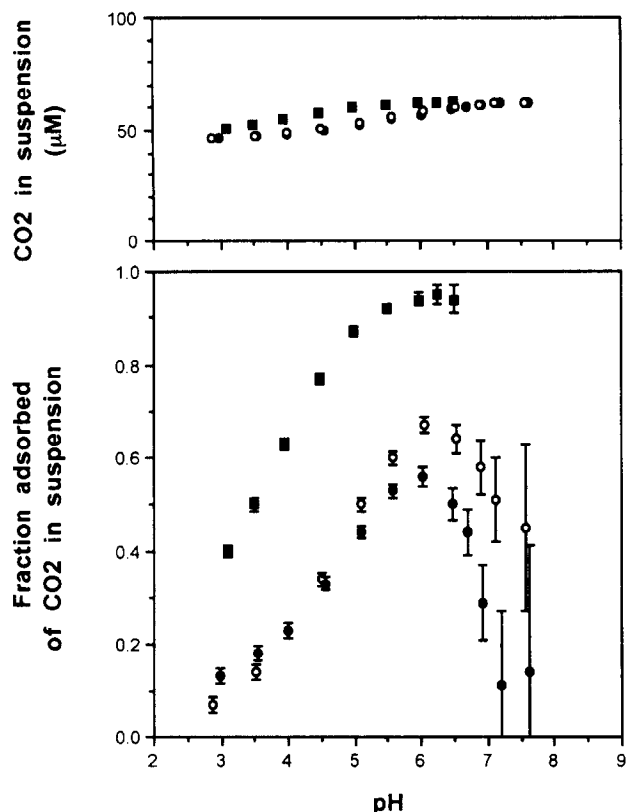


FIG. 4. Fraction adsorbed of total CO_2 in the solid suspension calculated from data in Fig. 3 and Eqn. 2 for 10 g/L (filled squares) and 2 g/L goethite (filled circles) in 0.1 N NaClO_4 . Open circles show adsorption for 2 g/L goethite suspension in 0.01 N NaClO_4 . Error bars calculated by propagating an $8 \mu\text{atm}$ uncertainty in the difference in headspace P_{CO_2} for the suspension and the solid free solution. Upper panel shows increases in total CO_2 in the suspension as a function of pH.

reflect insufficient precautions taken to exclude CO_2 . To our knowledge, our data show for the first time no evidence of hysteresis between the acid and base legs of potentiometric titrations for goethite. We attribute this to the rigorous efforts to exclude CO_2 . Note that if the change in surface charge density during a potentiometric titration is calculated from Eqn. 1, there is no need to invoke binding of carbonate species to explain a lower apparent pH_{pzc} for unpurged suspensions. Carbon dioxide in solution buffers the suspension towards a lower pH. Therefore, for a given amount of net acid added ($C_a - C_b$) to the suspension, the term $[\text{H}^+] - [\text{OH}^-]$ will be larger, leading to a lower apparent surface charge than for a CO_2 -free system. The cross-over point from a positively to a negatively charged surface will appear to occur at a lower pH.

There is as yet no consensus on a single model to interpret pH-surface charge density data such as shown in Fig. 2 in terms of formation of specific complexes at the metal oxide surface. As discussed by SPOSITO (1984), reactions at the surface of a crystalline solid such as goethite are difficult to describe because there are several types of functional groups with different tendencies to protonate and deprotonate. Models of an iron oxide surface typically bypass this problem assuming only a single type of amphoteric functional group

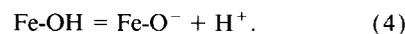
of the type Fe-OH. As clearly stated by DZOMBAK and MOREL (1990), all surface complexation models rest on the assumption that (1) sorption on oxides takes place at specific coordination sites, (2) sorption can be described quantitatively via mass law equations, (3) surface charge results from the sorption reactions, and (4) the effect of surface charge on sorption can be taken into account by applying a correction factor derived from electric double layer theory to mass law constants for surface reactions. The two models used here to evaluate carbonate species adsorption are the diffuse double layer model and the triple layer model. They differ only in their geometric representation of the diffuse layer of counter ions in solution induced by the charged oxide surface and the type of surface complexes allowed to form. SCHINDLER and KAMBER (1968), SCHINDLER and GAMSJÄGER (1972), and STUMM et al. (1970) wrote seminal papers leading to versions of the diffuse double layer model. YATES et al. (1974) and DAVIS et al. (1978) contributed to development of the triple-layer model. The main features of these two models are reviewed briefly before extracting the relevant surface complexation constants from the titration data.

Diffuse double-layer model

In this description, the oxide/water interface is composed of two layers of charge: a surface layer and a diffuse layer of counterions in solution. All specifically adsorbed ions are assigned to the surface layer. Electrolyte binding to the metal oxide surface is considered negligible and the dependence of surface charge on pH is attributed to protonation and deprotonation reactions of the surface sites:



and



Apparent equilibrium "constants" for these two surface species calculated from titration data as for a reaction in solution vary with pH because reactions 3 and 4 are affected by the variable charge of the oxide surface. As an oxide surface becomes protonated, repulsion from the positively charged surface makes additional protonation of surface sites less favorable. Conversely, as the oxide surface becomes negatively charged, more energy is required to dissociate a proton from the surface (DZOMBAK and MOREL, 1990). Potentiometric titration data of oxide surfaces have been modeled successfully if exponential coulombic corrections shown in Table 1 are included in the expression of intrinsic equilibrium constants for reactions 3 and 4. The Gouy-Chapman electrical double layer theory determines the relation between surface potential Ψ and surface charge. The infinite dilution reference state is used for aqueous species and a zero surface charge reference state is used for surface species (DZOMBAK and MOREL, 1990). Activity coefficients of surface species are assumed to be equal and cancel each other following the arguments of CHAN et al. (1975). The choice of activity coefficients for solutes entering the formation constant for adsorbed species differs from that advocated by HAYES and LECKIE (1987) and used by the speciation calculation program HYDRAQL (PAPELIS et al., 1988).

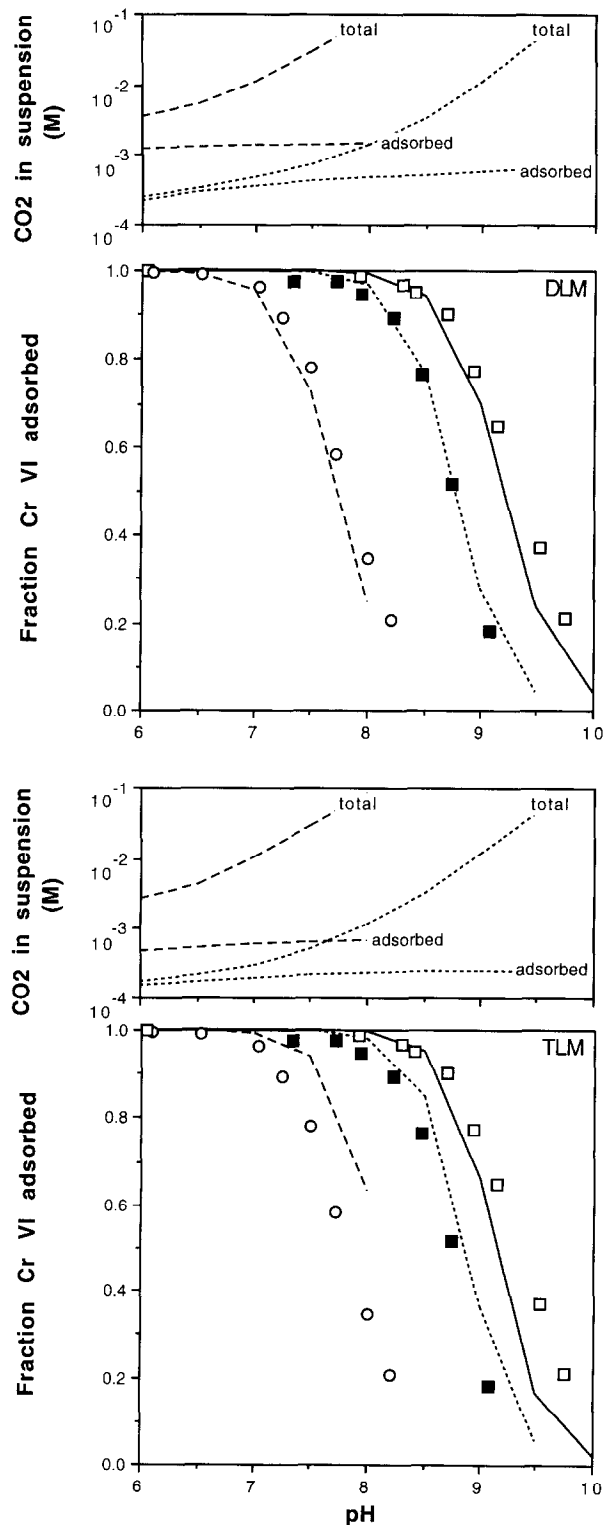


FIG. 5. Fraction of total Cr (VI) adsorbed as a function of pH for 10 g/L goethite in 0.1 N NaClO₄ for an open system under partial pressures of CO₂ < 5 μatm (open squares), 450 μatm (filled squares), and 40,000 μatm (open circles). Cr (VI) binding constant with determined with FITEQL from "CO₂-free" experiment. Best fit shown by solid line for diffuse double-layer model (upper panel) and triple layer model (lower panel) with constants listed in Table 1. The model predictions of Cr (VI) adsorption under 450 μatm CO₂ (dotted line) and 40,000 μatm CO₂ (dashed line) take into account carbonate binding determined independently. Also shown are model calculations

The generalized nonlinear least-squares optimization program FITEQL (WESTALL, 1982) was used to calculate the surface reaction constants that best fit the titration data. In the diffuse layer model, the only reaction considered in addition to protonation and deprotonation of the oxide surface is the dissociation of water. In FITEQL, mass actions laws are expressed in the tableau format of MOREL (1983). Other constraints imposed by FITEQL are the total number of sites for the oxide surface and the surface potential-charge relation. The total moles of acid/base added and pH data are also listed in an input file for FITEQL. The program calculates the formation constants for surface species Fe-OH₂⁺ and Fe-O⁻ that minimize the squared residuals between the acid/base added and the same model derived proton mass balance.

In setting up the input file for FITEQL, the suggestion of using surface site density of 2.31 sites/nm² for goethite by DAVIS and KENT (1990) was followed to facilitate the creation of a consistent set of intrinsic binding constants. This same surface site density was used by DZOMBAK and MOREL (1990) for amorphous iron oxyhydroxide. The site density is slightly lower than that estimated for goethite by various experimental methods (DAVIS and KENT, 1990) and geometrical considerations of the functional groups available in the crystal lattice (SPOSITO, 1984). Given a fixed site density, the only parameters that can be fitted to the titration data with the diffuse double-layer model are the formation constants for protonated and deprotonated surface sites. FITEQL was run in the "concentration mode" separately for the 0.10, 0.03, and 0.01 N ionic strength titration data (Appendix A), i.e., the water-dissociation (and later also carbonate-dissociation) constant was corrected to be valid for H⁺ and OH⁻ concentrations at the ionic strength of the titration, and pH data was converted to H⁺ concentrations. The intrinsic constants at infinite dilution listed in Table 1 are the mean of the intrinsic constants obtained at the three different ionic strength. Best fit intrinsic constants at individual ionic strengths differed by less than 0.19 and 0.23 log units for Fe-OH₂⁺ and Fe-O⁻, respectively. There is fair agreement between measured and model-predicted variation in surface charge density as a function of pH based on the constants in Table 1 for this model (Fig. 2).

Triple layer model

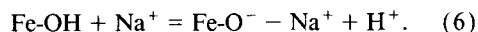
The main argument for considering electrolyte binding to the surface is that measurements of surface potential by electrophoresis are usually much lower than surface potentials calculated from titration data and double layer theory. It should be noted, however, that DZOMBAK and MOREL (1990) question this justification by citing the difficulty of interpreting electrophoresis experiments and the fact that the adsorption data for hydrous ferric oxide can adequately be modeled by their extension of the diffuse layer model. The triple-layer model distinguishes between adsorption at the oxide surface (inner-sphere complexes) and weaker, more ionic strength dependent, adsorption as outer-sphere complexes. A layer of water molecules separates weakly bound

of concentrations of total CO₂ in the suspension and CO₂ adsorbed onto goethite for both models at 450 μatm (dotted line) and 40,000 μatm (dashed line) CO₂. Formation of NaHCO₃ and NaCO₃ was taken into account in the modelling.

ions from the oxide surface (HAYES et al., 1987). Formation of the following surface complexes was proposed by YATES et al. (1974) and DAVIS et al. (1978) to account for the lower than expected charge of the diffuse layer of metal oxides that was measured:



and



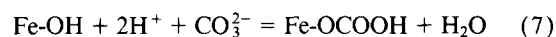
An inner- (C_1) and an outer-layer capacitance (C_2) determine the charge-potential relation for distinct regions of the diffuse layer where strongly and weakly bound ions are thought to be present. YATES et al. (1974) found it necessary to assume values of 1.4 and 0.2 F/m² for C_1 and C_2 , respectively, to obtain simultaneous agreement of the calculated surface charge and the diffuse layer potential with experimental values of surface charge and electrokinetic potential. The same value is used here for C_2 since it is reasonable for compact layer capacitance on Hg and AgI surfaces (LYKLEMA and OVERBEEK, 1961; STUMM et al., 1970). C_1 , however, is an adjustable parameter in the model over the range 0.1–2.0 F/m² (HAYES et al., 1991). The mean of the absolute values of the formation constants for protonated and deprotonated sites is usually constrained by $\text{pH}_{\text{pzc}} = (|\text{pKFeOH}_2^+| + |\text{pKFeO}^-|)/2$ to determine formation constants for complexes $\text{Fe-OH}_2^+ - \text{ClO}_4^-$ and $\text{Fe-O}^- - \text{Na}^+$ from titration data. The difference between $|\text{pKFeOH}_2^+|$ and $|\text{pKFeO}^-|$ (i.e., ΔpK_a), however, is a second adjustable parameter of the model. The site density of the goethite surface is kept at 2.3 sites/nm². After running FITEQL with various possible combinations of values for C_1 and ΔpK_a , we found that the goethite titration data in Appendix A are fitted best for $C_1 = 1.5$ F/m². No significant differences in the fit was found for ΔpK_a values of 1, 2, 3, and 4. These results are consistent with the conclusions of WESTALL and HOHL (1980) and HAYES et al. (1991) that potentiometric data can often be fitted equally well with a relatively wide range of internally consistent parameters. The variation of surface charge density as a function of pH predicted by the triple-layer model for the formation constants and parameters listed in Table 1 ($\Delta\text{pK}_a = 2$) agrees well with the data (Fig. 2).

Carbonate Species Adsorption

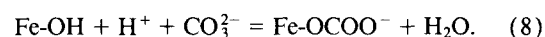
Maximum adsorption of carbonate species onto goethite at intermediate pH observed in our data may be representative of the behaviour of carboxylic acid functional groups. Similar behaviour has been observed for carbonic and acetic acid adsorption on aluminum oxide (SCHULTHESS and MCCARTHY, 1990), and natural humic matter on alumina (DAVIS, 1982). Our data can more directly be compared with the carbonate adsorption data of ZACHARA et al. (1987) for amorphous ferric hydroxide determined with ¹⁴C-labelled bicarbonate. The general trend of their results suggest a maximum fraction adsorbed $f_{\text{max}} \sim 0.5$ of carbonate species in the suspension adsorbed for a surface site concentration of $\sim 1.8 \cdot 10^{-4}$ M (calculated from $0.87 \cdot 10^{-3}$ M Fe_T , 600 m²/g surface area, and 2.3 sites/nm²). Comparison with our goethite data ($f_{\text{max}} = 0.56$, 2 g/L, $\sim 3.4 \cdot 10^{-4}$ M of sites) and

our unpublished hematite data ($f_{\text{max}} = 0.80$, 5.75 g/L, $3.1 \cdot 10^{-4}$ M sites) suggests that binding of carbonate species is comparable on a per site basis for different iron oxides.

Infrared absorption studies of CO₂ adsorption on goethite suggest that coordination interaction takes place at the oxide surface (RUSSELL et al., 1974; ZELTNER and ANDERSON, 1988; YAPP and POTHS, 1990). Binding of carbonate species to the goethite surface may be similar to that observed for another oxyanion, selenite (SeO_3^{2-}), by in situ extended X-ray absorption fine structure measurements (HAYES et al., 1987). If carbonate species indeed bind as inner-sphere complexes to the goethite surface, it is reasonable to postulate two surface complex stoichiometries, one protonated and one deprotonated:



and



The reactions are written in terms of carbonate because it is the component added to the FITEQL format. The two reactions amount to replacing an Fe-bound surface hydroxyl with a more acidic carboxylic group and would, therefore, tend to lower the pH_{pzc} of the suspension. For the surface complex containing a protonated carboxylic group, there is no electrostatic contribution to the free energy of this reaction. The expressions for the formation constant of both surface species are the same for the diffuse-layer model and the triple-layer model (Table 1). The carbonate species adsorption data at 0.1 N NaClO₄ was recalculated in terms of free carbonate concentration (Appendix B) and entered into the FITEQL format as a function of proton concentration, together with the formation constants for bicarbonate and carbonic acid (Table 1). For all FITEQL calculations, a constant total concentration of $5.5 \cdot 10^{-5}$ M of CO₂ in the suspension was assumed for simplicity. The effect of changing total CO₂ in the range shown in Fig. 4 on the calculated fraction adsorbed is minimal. Comparison of the carbonate adsorption data with the model results from the formation constants in Table 1 show that both the diffuse layer and the triple layer model can reproduce the distinct maximum observed around pH 6 (Fig. 6).

For the final model runs, only the 2 g/L and 10 g/L data in 0.1 N NaClO₄ at pH > 5 were used to obtain the best fit formation constants in the pH range most relevant to natural waters. Carbonate adsorption data with large error bars (2 g/L, 0.1 N, pH 7.19 and 7.61) were also excluded from the regression. Intrinsic formation constants listed in Table 1 are the average of constants obtained for the 2 and 10 g/L suspensions in 0.1 N NaClO₄. In the case of the diffuse layer model, the model-derived contributions from the protonated and deprotonated species are about equal at pH 6. For the triple-layer model, the regression does not converge if both species are considered. A good fit to the data is obtained, however, if only the deprotonated carbonate surface complex is considered. While the potentiometric titration data does not constrain the ΔpK_a value for complexes Fe-OH_2^+ and Fe-O^- , FITEQL regressions of the carbonate adsorption do yield a slightly better fit for $\Delta\text{pK}_a = 2$ than for $\Delta\text{pK}_a = 1, 3, 4$. This criterion was the basis for the selecting the triple-layer

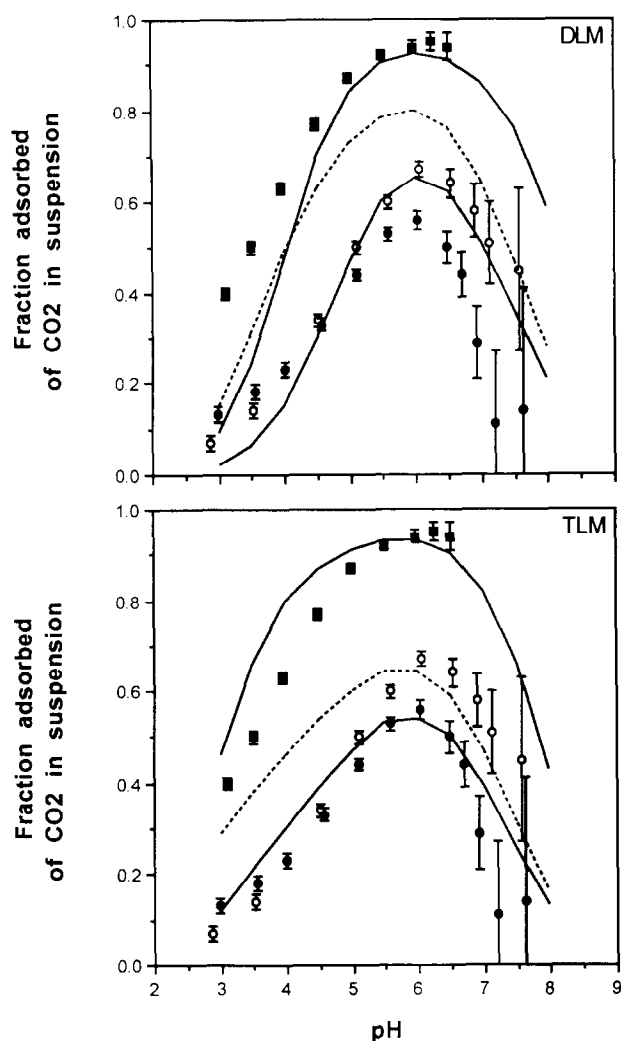


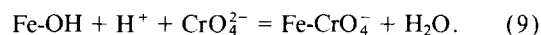
FIG. 6. Comparison of carbonate species adsorption data with model predictions for the diffuse double-layer model (upper panel) and the triple-layer model (lower panel) in 0.1 N NaClO₄ from the formation constants listed in Table 1. Goethite concentrations of 2 g/L (circles) and 10 g/L (filled squares). Dotted line shows model prediction of carbonate adsorption for 2 g/L goethite in 0.01 N NaClO₄ (open circles).

model parameters in Table 1. Carbonate species adsorption at the lower ionic strength of 0.01 N NaClO₄ was predicted from the intrinsic constants in Table 1 following appropriate activity corrections. The results are consistent with the modest increase in the fraction of carbonate species adsorbed that is observed at pH > 5 (Fig. 6). Both the diffuse-layer and the triple-layer model significantly overestimate the sensitivity of carbonate adsorption at pH < 5.

Competition for Surface Sites Between Carbonate and Other Ions

The carbonate species surface complexation constants can be used to predict the effect of increasing the partial pressure of CO₂ in the chromate adsorption experiments. The "carbonate-free" chromate adsorption data (Appendix C) was fitted with FITEQL for both the diffuse double-layer and the

triple layer model considering the same complex stoichiometry:



In the case of the triple layer model, the binding constant listed in Table 1 represents the formation of an inner-sphere complex. It is reasonable to assume that the chromate ion forms the same type of surface complex as carbonate since the presence of 10⁻² M Cr (IV) prevents carbonate from adsorbing onto goethite (Fig. 3). The predicted reductions in chromate adsorption following equilibration with 450 and 40,000 μatm CO₂ are very close to the observations in the case of the diffuse double-layer model (Fig. 5). The model therefore suggests that it is surface coverage by adsorbed carbonate species that causes the chromate adsorption edge to shift. Extensive coverage by carbonate species means both that there are fewer sites available and that the surface potential is less favorable for chromate adsorption. It is useful to note that at a given P_{CO2}, the absolute concentration of bound carbonate species calculated from the model increases by less than a factor of three from pH 6 to 9 (Fig. 5). This is because the effect of decreasing the fraction of carbonate species adsorbed as the pH rises is compensated by the increase in total CO₂ in solution under a fixed partial pressure of CO₂. The carbonate surface coverage predicted by the triple layer model is consistently lower than that predicted by the diffuse double-layer model. This probably accounts for the smaller shift in the chromate pH adsorption edge predicted by the triple layer model (Fig. 5). In comparing the two models, it must be noted that two carbonate sorption reactions were included for the diffuse double-layer model and only one for the triple layer model (Table 1). FITEQL did not converge to a solution when two reactions were considered for the triple layer model. In the closed system experiments, the fraction of the goethite surface sites bound to CO₂ was less than 0.1. At higher surface coverage, a neutral carbonate-surface site complex is likely to be more important. Inclusion of a neutral carbonate surface complex in the triple layer model might increase predicted goethite surface coverage by carbonate, and therefore might increase the predicted chromate adsorption edge shift.

The ability of the models to simulate chromate binding data in the open system at widely different P_{CO2} with stoichiometries and constants derived from low carbonate surface coverage experiments suggests that the carbonate binding constants in Table 1 are applicable to natural systems. Goethite is the dominant iron oxide found in soils. In addition, carbonate species binding to other iron oxides on a per site basis (hydrated ferric oxide or hematite) appears to be comparable. Figure 7 is a compilation of model calculations for the fraction of goethite-like surface sites bound to carbonate species for an open system. Results are shown for both the diffuse double-layer model and the triple layer model based on the carbonate binding constants listed in Table 1. The diffuse double-layer model predicts that the fraction of goethite-like surface sites bound to CO₂ in a 0.1 N ionic strength suspension typically ranges between 0.04 (pH 5 and 350 μatm CO₂) and 0.84 (pH 8 and 35,000 μatm CO₂). The reactive surface sites of natural iron hydroxides may well be predominantly covered by carbonate species.

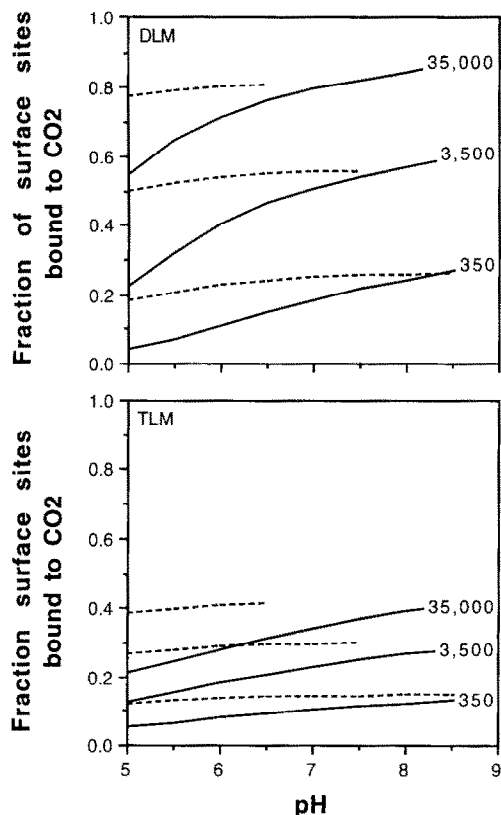


FIG. 7. Model calculation of the fraction of total goethite-like sites bound to CO_2 as a function of pH at CO_2 partial pressures of 350, 3,500, 35,000 μatm in 0.1 N (solid line) and 0.001 N (dashed line) ionic strength suspensions. Upper panel shows results for diffuse double-layer model, lower panel for triple layer model. Dashed lines end where the ionic strength increases above 0.002 N due to rising CO_2 in solution. These calculations are independent of the solid concentration in the suspension because total carbonate in solution is determined by the partial pressure of CO_2 . Formation of NaHCO_3 and NaCO_3 was taken into account in the modelling.

CONCLUSIONS

The pH_{pzc} of a goethite suspension measured by potentiometric titration in NaClO_4 is 8.9, a value significantly higher than reported in a number of previous studies. No hysteresis was observed between the acid and base legs of the titration perhaps because particular care was taken to limit introduction of CO_2 in the suspension. The triple layer model fits the potentiometric titration data over a wider pH range than the diffuse double-layer model.

Adsorption of carbonate species onto metal oxide particles can be determined by measuring headspace P_{CO_2} in equilibrium with a solid suspension. One advantage of this method over using ^{14}C -labelled bicarbonate is that exchange of CO_2 with the surroundings can be monitored and prevented. For a fixed total amount CO_2 in the suspension, adsorption of carbonate species onto goethite shows a well-developed maximum at $\text{pH} \sim 6$. This feature can be modelled with both the diffuse double-layer and the triple layer model. Modelling of the reduction in chromate adsorption at elevated partial pressures of CO_2 suggests that the formation constants de-

termined for carbonate surface complexes can be extrapolated to $\text{pH} > 7$ and higher surface coverage. Our results suggest that metal oxide surface sites that determine partitioning of metal ions between the dissolved and the particulate phase in natural waters may be largely bound to carbonate species. The pH dependence of carbonate binding to iron oxide surfaces may also have to be taken into account when past atmospheric CO_2 is inferred from the carbonate content of goethite in ancient rock formations (YAPP and POTHS, 1992).

Acknowledgments—Jan van Gestel, late glassblower of the Chemistry Department, skillfully made the equilibration vessel. We thank John Hessler for adapting the pump to a different motor. This work was funded in part by the Electric Power Research Institute, Los Alamos Contract 9X69-1818X-1, and a NATO postdoctoral fellowship to A.v.G obtained with the help of Jean-Marie Martin at the Institut de Biogéochimie Marine, Ecole Normale Supérieure (France). We also thank Chris Fuller of the USGS, Menlo Park, CA, USA, for access to counting equipment. Discussions with Matthias Kohler were fruitful throughout the experimental work and the preparation of the manuscript. We thank L. Charlet and two anonymous reviewers for their comments. The code FITEQL used for data analysis has not been fully qualified per the Yucca Mountain Site Characterization Project Software Quality Assurance Plan.

Editorial handling: G. Sposito

REFERENCES

- ATKINSON F. J., POSNER A. M., and QUIRK J. P. (1967) Adsorption of potential determining ions at the ferric oxide-aqueous electrolyte interface. *J. Phys. Chem.* **71**, 550–558.
- BALISTRERI L. S. and MURRAY J. W. (1982) The surface chemistry of delta- MnO_2 in major ion seawater. *Geochim. Cosmochim. Acta* **46**, 1041–1052.
- BALISTRERI L. S. and MURRAY J. W. (1983) Metal-solid interactions in the marine environment: Estimating apparent equilibrium binding constants. *Geochim. Cosmochim. Acta* **47**, 1091–1098.
- BENJAMIN M. M. (1983) Adsorption and surface precipitation of metals on amorphous iron oxyhydroxide. *Environ. Sci. Technol.* **17**, 686–692.
- BENJAMIN M. M. and LECKIE J. O. (1982) Effects of complexation by Cl , SO_4 , and S_2O_3 on the adsorption behaviour of cadmium on oxide surfaces. *Environ. Sci. Tech.* **16**, 162–170.
- BOURG A. C. M. and SCHINDLER P. W. (1978) Ternary surface complexes I. Complex formation in the system silica-Cu(II)-ethylenediamine. *Chimia* **32**, 166–168.
- BRUNAUER S., EMMETT P. H., and TELLER E. (1938) Adsorption of gases in multimolecular layers. *J. Phys. Chem.* **60**, 309–319.
- BRUNO J., STUMM W., WERSIN P., and BRANDBERG F. (1992) On the influence of carbonate in mineral dissolution: I. The thermodynamics and kinetics of hematite dissolution in bicarbonate solutions at $T = 25^\circ\text{C}$. *Geochim. Cosmochim. Acta* **56**, 1139–1147.
- VAN CAPPELLEN P., CHARLET L., STUMM W., and WERSIN P. (1993) A surface complexation model of the carbonate mineral-aqueous solution interface. *Geochim. Cosmochim. Acta* **57**, 3505–3518.
- CHAN D., PERRAM J. W., WHITE L. R., and HEALY T. W. (1975) Regulation of surface potential amphoteric surfaces during particle-particle interaction. *J. Chem. Soc., Faraday Trans. 1*, **71**, 1046–1057.
- CHISHOLM-BRAUSE C. J., HAYES K. F., ROE A. L., BROWN G. E., JR., PARKS G. A., and LECKIE J. O. (1990) Spectroscopic investigations of Pb(II) complexes at the $\alpha\text{-Al}_2\text{O}_3$ /water interface. *Geochim. Cosmochim. Acta* **54**, 1897–1909.
- COMBES J. M., CHISHOLM-BRAUSE C. J., BROWN G. E., JR., and PARKS G. A. (1992) EXAFS spectroscopic study of neptunium (V) sorption at the $\alpha\text{-FeOOH}$ /water interface. *Environ. Sci. Technol.* **26**, 376–382.
- DAVIS J. A. (1982) Adsorption of natural dissolved organic matter at the oxide/water interface. *Geochim. Cosmochim. Acta* **46**, 2381–2393.

- DAVIS J. A. and KENT D. B. (1990) Surface complexation modeling in aqueous geochemistry. In *Mineral-Water Interface Geochemistry* (ed. M. F. HOCELLA and A. F. WHITE); *Rev. Mineral.* **23**, pp. 177–260. Mineral. Soc. Amer.
- DAVIS J. A. and LECKIE J. O. (1978) Surface ionization and complexation at the oxide/water interface. II. Surface properties of amorphous iron oxyhydroxide and adsorption of metal ions. *J. Colloid Interface Sci.* **67**, 90–107.
- DAVIS J. A. and LECKIE J. O. (1980) Surface ionization and complexation at the oxide/water interface. III. Adsorption of anions. *J. Colloid Interface Sci.* **74**, 32–43.
- DAVIS J. A., JAMES R. O., and LECKIE J. O. (1978) Surface ionization and complexation at the oxide/water interface. I. Computation of double-layer properties in simple electrolytes. *J. Colloid Interface Sci.* **63**, 480–499.
- DZOMBACK D. A. and MOREL F. M. M. (1990) *Surface Complexation Modeling: Hydrous Ferric Oxide*. Wiley.
- FULLER C. C. and DAVIS J. A. (1987) Processes and kinetics of Cd⁺² sorption by a calcareous aquifer sand. *Geochim. Cosmochim. Acta* **51**, 1491–1502.
- HARNED H. S. and DAVIS R. D., JR. (1943) The ionization constant of carbonic acid in water and the solubility of carbon dioxide in water and aqueous salt solutions from 0 to 50°. *Anal. Chem.* **65**, 2030–2037.
- HAYES K. F. and LECKIE J. O. (1987) Modeling ionic strength effects on cation adsorption at hydrous oxide/solution interfaces. *J. Colloid Interface Sci.* **115**, 564–572.
- HAYES K. F., ROE A. L., BROWN G. E., HODGSON K. O., LECKIE J. O., and PARKS G. A. (1987) In situ X-ray adsorption study of surface complexes: Selenium oxyanions on α -FeOOH. *Science* **238**, 783–786.
- HAYES K. F., PAPELIS C., and LECKIE J. O. (1988) Modeling ionic strength effects on anion adsorption at hydrous oxide/solution interfaces. *J. Colloid Interface Sci.* **125**, 717–726.
- HAYES K. F., REDDEN G., ELA W., and LECKIE J. O. (1991) Surface complexation models: An evaluation of model parameter estimations using FITEQL and oxide mineral titration data. *J. Colloid Interface Sci.* **142**, 448–469.
- HEM J. D. (1970) Study and interpretation of the chemical characteristics of natural water. *Geological Survey Water-Supply Paper 1473* (2nd. ed.).
- HOLLAND H. D. (1978) *The Chemistry of the Atmosphere and Oceans*. Wiley.
- HUANG C. P. and STUMM W. (1973) Specific adsorption of cations on hydrous α -Al₂O₃. *J. Colloid Interface Sci.* **22**, 231–259.
- JAMES R. O. and PARKS G. A. (1982) *Characterization of aqueous colloids by their electrical double layer and intrinsic surface chemical properties*, *Surface and Colloid Science*, Vol. 12, (ed. MATIJEVIC E.)
- LYKLEMA J. and OVERBEEK J. T. G. (1961) The capacity of the double layer at the silver iodide/water interface. *J. Coll. Sci.* **16**, 595.
- MOREL F. M. M. (1983) *Principles of Aquatic Chemistry*. Wiley.
- PAPELIS C., HAYES K. F., and LECKIE J. O. (1988) *HYDRAQL: A program for the computation of aqueous batch systems including surface-complexation modeling of ion adsorption at the oxide/solution interface*. Technical Report 306, Dept. of Civil Engineering, Stanford Univ.
- ROE A. L., HAYES K. F., CHISHOLM-BRAUSE C., BROWN G. E., PARKS G. A., HODGSON K. O., and LECKIE J. O. (1991) In situ X-ray adsorption study of lead ion surface complexes at the goethite-water interface. *Langmuir* **7**, 367–373.
- RUSSELL J. D., PATTERSON E., FRASER A. R., and FARMER, V. C. (1974) Adsorption of carbon dioxide on goethite (α -FeOOH) surfaces, and its implications for anion adsorption. *Adv. Colloid Sci.* **52**, 1623–1630.
- SCHINDLER P. W. and GAMSJÄGER H. (1972) Acid-base reactions of the TiO₂ (anatase)-water interface and the point of zero charge of TiO₂ suspensions. *Kolloid Z. Z. Polymere* **250**, 759–763.
- SCHINDLER P. W. and STUMM W. (1987) The surface chemistry of oxides, hydroxides, and oxide minerals. In *Aquatic Surface Chemistry* (ed. W. STUMM), pp. 83–110. Wiley.
- SCHINDLER P. W. and KAMBER H. R. (1968) Die Acidität von Silanolgruppen. *Helv. Chim. Acta* **51**, 1781–1786.
- SCHULTHESS C. P. and MCCARTHY J. F. (1990) Competitive adsorption of aqueous carbonic and acetic acids by an aluminum oxide. *Soil Sci. Soc. Amer. J.* **54**, 688–694.
- SHILLER A. M. and BOYLE E. A. (1987) Variability of dissolved trace metals in the Mississippi River. *Geochim. Cosmochim. Acta* **51**, 3273–3277.
- SPOSITO G. (1984) *The Surface Chemistry of Soils*. Oxford Univ. Press.
- SPOSITO G. (1989) *The Chemistry of Soils*. Oxford Univ. Press.
- STUMM W. and MORGAN J. J. (1981) *Aquatic Chemistry*, 2nd ed. Wiley.
- STUMM W., HUANG C. P., and JENKINS S. R. (1970) Specific chemical interactions affecting the stability of dispersed systems. *Croat. Chem. Acta* **42**, 223–244.
- TUREKIAN K. K. (1977) The fate of metals in the ocean. *Geochim. Cosmochim. Acta* **41**, 1139–1144.
- WESTALL J. C. (1982) *FITEQL: A program for the determination of chemical equilibrium constants from experimental data*. Technical report 82.02, Dept. Chem., Oregon State Univ., Corvallis, OR, USA.
- WESTALL J. C. and HOHL H. (1980) A comparison of electrostatic models for the oxide/solution interface. *Adv. Colloid Interface Sci.* **12**, 265–294.
- WIELAND E. and STUMM W. (1992) Dissolution kinetics of kaolinite in acidic aqueous solutions at 25°C. *Geochim. Cosmochim. Acta* **56**, 3339–3355.
- YAPP C. J. and POTHS H. (1990) Infrared spectral evidence for a minor Fe (111) carbonate-bearing component in a natural goethite. *Clays Clay Mineral.* **38**, 442–444.
- YAPP C. J. and POTHS H. (1992) Ancient atmospheric CO₂ pressures inferred from natural goethite. *Nature* **355**, 342–344.
- YATES D. E. and HEALY T. W. (1975) Mechanism of anion adsorption at the ferric and chromic oxide/water interfaces. *J. Colloid Interface Sci.* **52**, 222–228.
- YATES D. E., LEVINE S., and HEALY T. W. (1974) Site-binding model of the electrical double layer at the oxide/water interface. *J. Chem. Soc. Faraday Trans. I*, **70**, 1807–1818.
- ZACHARA J. M., GIRVIN D. C., SCHMIDT R. L., and RESCH C. T. (1987) Chromate adsorption on amorphous iron oxyhydroxide in the presence of major groundwater ions. *Environ. Sci. Tech.* **21**, 589–594.
- ZELTNER W. A. and ANDERSON M. A. (1988) Surface charge development at the goethite/aqueous solution interface: Effects of CO₂ adsorption. *Langmuir* **4**, 469–474.

Appendix A.

pH	Moles acid	Volume (L)	NaClO ₄ (N)	pH	Moles acid	Volume (L)	NaClO ₄ (N)	pH	Moles acid	Volume (L)	NaClO ₄ (N)
4.65	9.33e-5	0.100	0.010	4.92	9.33e-5	0.100	0.030	5.34	9.33e-5	0.100	0.100
4.86	8.54e-5	0.100	0.010	5.09	8.72e-5	0.100	0.030	5.53	8.72e-5	0.100	0.100
5.08	7.77e-5	0.100	0.010	5.27	8.11e-5	0.100	0.030	5.72	8.11e-5	0.100	0.100
5.31	7.01e-5	0.100	0.010	5.46	7.50e-5	0.100	0.030	5.91	7.50e-5	0.100	0.100
5.55	6.25e-5	0.100	0.010	5.65	6.89e-5	0.100	0.030	6.10	6.89e-5	0.100	0.100
5.80	5.48e-5	0.100	0.010	5.86	6.28e-5	0.100	0.030	6.31	6.28e-5	0.100	0.100
6.02	4.87e-5	0.100	0.010	6.07	5.67e-5	0.100	0.030	6.52	5.67e-5	0.100	0.100
6.25	4.26e-5	0.100	0.010	6.29	5.06e-5	0.100	0.030	6.74	5.06e-5	0.100	0.100
6.50	3.65e-5	0.100	0.010	6.48	4.57e-5	0.100	0.030	6.97	4.45e-5	0.100	0.100
6.72	3.16e-5	0.100	0.010	6.66	4.11e-5	0.100	0.030	7.15	3.96e-5	0.100	0.100
6.95	2.71e-5	0.100	0.010	6.85	3.65e-5	0.100	0.030	7.34	3.50e-5	0.100	0.100
7.19	2.25e-5	0.100	0.010	7.05	3.19e-5	0.100	0.030	7.53	3.04e-5	0.100	0.100
7.41	1.88e-5	0.100	0.010	7.27	2.74e-5	0.100	0.030	7.72	2.58e-5	0.100	0.100
7.66	1.52e-5	0.100	0.010	7.45	2.37e-5	0.100	0.030	7.91	2.13e-5	0.100	0.100
7.85	1.21e-5	0.100	0.010	7.64	2.00e-5	0.100	0.030	8.12	1.67e-5	0.100	0.100
8.09	9.04e-6	0.100	0.010	7.85	1.64e-5	0.100	0.030	8.32	1.21e-5	0.100	0.100
8.33	5.99e-6	0.100	0.010	8.03	1.33e-5	0.100	0.030	8.52	7.51e-6	0.100	0.100
8.54	3.54e-6	0.100	0.010	8.22	1.03e-5	0.100	0.030	8.72	2.93e-6	0.100	0.100
8.77	7.94e-7	0.100	0.010	8.40	7.21e-6	0.100	0.030	8.91	-1.65e-6	0.100	0.100
8.98	-1.95e-6	0.100	0.010	8.59	4.15e-6	0.100	0.030	9.08	-6.23e-6	0.100	0.100
9.19	-5.31e-6	0.100	0.010	8.77	1.10e-6	0.100	0.030	9.27	-1.17e-5	0.100	0.100
9.41	-9.59e-6	0.100	0.010	8.94	-1.95e-6	0.100	0.030	9.44	-1.72e-5	0.100	0.100
9.62	-1.48e-5	0.100	0.011	9.12	-5.62e-6	0.100	0.030	9.61	-2.36e-5	0.100	0.100
9.86	-2.24e-5	0.100	0.011	9.31	-9.90e-6	0.100	0.030	9.78	-3.10e-5	0.100	0.100
10.09	-3.31e-5	0.100	0.011	9.51	-1.51e-5	0.100	0.030	9.98	-4.14e-5	0.100	0.100
10.31	-4.81e-5	0.100	0.011	9.69	-2.06e-5	0.100	0.030	10.17	-5.42e-5	0.100	0.100
10.53	-7.13e-5	0.101	0.011	9.88	-2.82e-5	0.100	0.031	10.36	-7.13e-5	0.101	0.100
10.74	-1.03e-4	0.101	0.011	10.07	-3.74e-5	0.100	0.031	10.55	-9.48e-5	0.101	0.101
10.52	-7.05e-5	0.101	0.011	10.26	-5.02e-5	0.100	0.031	10.74	-1.27e-4	0.101	0.101
10.25	-4.42e-5	0.101	0.011	10.45	-6.73e-5	0.101	0.031	10.92	-1.72e-4	0.101	0.101
10.00	-2.92e-5	0.101	0.011	10.64	-9.08e-5	0.101	0.031	10.73	-1.24e-4	0.101	0.101
9.72	-1.79e-5	0.101	0.011	10.82	-1.23e-4	0.101	0.031	10.49	-8.63e-5	0.101	0.101
9.48	-1.14e-5	0.101	0.011	10.62	-8.79e-5	0.101	0.031	10.29	-6.38e-5	0.101	0.101
9.24	-6.35e-6	0.101	0.011	10.38	-6.03e-5	0.101	0.031	10.06	-4.63e-5	0.101	0.101
9.03	-2.59e-6	0.101	0.011	10.18	-4.44e-5	0.101	0.031	9.89	-3.60e-5	0.101	0.101
8.81	5.35e-7	0.101	0.011	9.96	-3.18e-5	0.101	0.031	9.69	-2.66e-5	0.101	0.101
8.56	3.66e-6	0.101	0.011	9.72	-2.18e-5	0.101	0.031	9.50	-1.91e-5	0.101	0.101
8.31	6.79e-6	0.101	0.011	9.55	-1.62e-5	0.101	0.031	9.32	-1.28e-5	0.101	0.101
8.06	9.92e-6	0.101	0.011	9.35	-1.06e-5	0.101	0.031	9.11	-6.55e-6	0.101	0.101
7.83	1.31e-5	0.101	0.011	9.15	-5.87e-6	0.101	0.031	8.93	-1.54e-6	0.101	0.101
7.61	1.62e-5	0.101	0.011	8.95	-2.11e-6	0.101	0.031	8.74	3.15e-6	0.101	0.101
7.37	1.99e-5	0.101	0.011	8.75	1.64e-6	0.101	0.031	8.54	7.85e-6	0.101	0.101
7.12	2.43e-5	0.101	0.011	8.57	4.77e-6	0.101	0.031	8.34	1.25e-5	0.101	0.101
6.90	2.87e-5	0.101	0.012	8.38	7.90e-6	0.101	0.031	8.13	1.72e-5	0.101	0.101
6.65	3.40e-5	0.101	0.012	8.18	1.10e-5	0.101	0.031	7.92	2.19e-5	0.101	0.101
6.41	3.96e-5	0.101	0.012	7.99	1.42e-5	0.101	0.031	7.72	2.66e-5	0.102	0.101
6.19	4.53e-5	0.101	0.012	7.81	1.73e-5	0.101	0.031	7.52	3.13e-5	0.102	0.101
5.98	5.09e-5	0.101	0.012	7.61	2.10e-5	0.101	0.031	7.33	3.60e-5	0.102	0.101
5.76	5.75e-5	0.101	0.012	7.42	2.48e-5	0.101	0.031	7.14	4.07e-5	0.102	0.101
5.52	6.50e-5	0.101	0.012	7.23	2.86e-5	0.101	0.031	6.93	4.63e-5	0.102	0.101
5.29	7.25e-5	0.101	0.012	7.03	3.29e-5	0.101	0.031	6.73	5.20e-5	0.102	0.101
5.08	8.00e-5	0.101	0.012	6.84	3.73e-5	0.101	0.031	6.53	5.76e-5	0.102	0.101
4.84	8.88e-5	0.101	0.012	6.66	4.17e-5	0.101	0.032	6.34	6.32e-5	0.102	0.101
4.61	9.82e-5	0.101	0.012	6.45	4.70e-5	0.101	0.032	6.15	6.89e-5	0.102	0.101
4.41	1.07e-4	0.101	0.012	6.25	5.26e-5	0.101	0.032	5.97	7.45e-5	0.102	0.101
4.19	1.19e-4	0.101	0.012	6.05	5.83e-5	0.101	0.032	5.80	8.01e-5	0.102	0.101
3.98	1.32e-4	0.101	0.012	5.86	6.39e-5	0.101	0.032	5.63	8.58e-5	0.102	0.101
				5.68	6.95e-5	0.101	0.032	5.45	9.23e-5	0.102	0.101
				5.52	7.52e-5	0.101	0.032	5.28	9.86e-5	0.102	0.101
				5.33	8.17e-5	0.101	0.032	5.12	1.05e-4	0.102	0.101
				5.16	8.80e-5	0.101	0.032	4.93	1.12e-4	0.102	0.101
				5.00	9.43e-5	0.101	0.032	4.74	1.20e-4	0.102	0.101
				4.81	1.02e-4	0.101	0.032	4.57	1.27e-4	0.102	0.101
				4.63	1.09e-4	0.101	0.032	4.39	1.36e-4	0.102	0.101
				4.44	1.18e-4	0.101	0.032	4.21	1.45e-4	0.102	0.101
				4.26	1.27e-4	0.102	0.032	4.03	1.57e-4	0.102	0.101
				4.06	1.39e-4	0.102	0.032				

Appendix.B

pH PCO2 f log[CO3-2]				pH PCO2 f log[CO3-2]				pH PCO2 f		
0.1 N 2 g/L		55 μM		0.1 N 10 g/L		55 μM		0.01 N 2 g/L		
2.99	1178	0.13		3.11	883	0.40		2.87	1183	0.07
3.54	1115	0.18		3.49	758	0.50		3.53	1097	0.14
4.00	1033	0.23		3.93	576	0.63		4.00	1005	0.23
4.57	911	0.33		4.46	365	0.77	-12.22	4.49	872	0.34
5.09	750	0.44	-10.60	4.98	210	0.87	-11.45	5.10	662	0.50
5.56	575	0.53	-9.79	5.49	116	0.92	-10.69	5.56	501	0.60
6.03	407	0.56	-9.00	5.97	62	0.94	-9.97	6.06	328	0.67
6.48	255	0.50	-8.28	6.25	41	0.95	-9.60	6.53	190	0.64
6.70	189	0.44	-7.94	6.51	33	0.94	-9.16	6.90	117	0.58
6.93	143	0.29	-7.56	3.20	859			7.11	90	0.51
7.19	94	0.11						7.56	50	0.45
7.61	52	0.14						2.95	1104	
3.04	1161									

Appendix.C

pH f Cr VI		pH f Cr VI		pH f Cr VI		log[CrO4-2]		
0.1 N Cr VI 5 10-6 M		10 g/L		450 μatm		<5 μatm		
PCO2	6.09	1.00	PCO2	7.34	0.97	PCO2	6.05	1.00
40,000 μatm	6.53	0.99	450 μatm	7.71	0.97	<5 μatm	7.92	0.99
	7.03	0.96		7.94	0.95		8.30	0.97
	7.24	0.89		8.23	0.89		8.41	0.95
	7.50	0.78		8.47	0.76		8.70	0.90
	7.71	0.58		8.75	0.52		8.94	0.77
	8.00	0.35		9.08	0.18		9.15	0.65
	8.21	0.21					9.53	0.37
							9.75	0.21
							10.05	0.18
								-7.81
								-8.19
								-8.30
								-8.59
								-8.83
								-9.04
								-9.42
								-9.64
								-9.94